Comparison of nonequilibrium processes in p + Ni and p + Au collisions at GeV energies

A. Budzanowski,[1] M. Fidelus,[2] D. Filges,[3] F. Goldenbaum,[3] H. Hodde,[4] L. Jarczyk,[2] B. Kamys,[2,*] M. Kistryn,[1] St. Kistryn,[2] St. Kliczewski,[1] A. Kowalczyk,[2] E. Kozik,[1] P. Kulessa,[1,3] H. Machner,[3] A. Magiera,[2] B. Piskor-Ignatowicz,[2,3] K. Pysz,[1,3] Z. Rudy,[2] R. Siudak,[1,3] and M. Wojciechowski[2]
(PISA Collaboration)
[1]*H. Niewodniczański Institute of Nuclear Physics PAN, Radzikowskiego 152, PL-31342 Kraków, Poland*
[2]*M. Smoluchowski Institute of Physics, Jagellonian University, Reymonta 4, PL-30059 Kraków, Poland*
[3]*Institut für Kernphysik, Forschungszentrum Jülich, D-52425 Jülich, Germany*
[4]*Institut für Strahlen- und Kernphysik, Bonn University, D-53121 Bonn, Germany*
(Received 1 September 2009; revised manuscript received 28 July 2010; published 15 September 2010)

The energy and angular dependence of double differential cross sections $d^2\sigma/d\Omega dE$ were measured for p, d, t, ^{3,4,6}He, ^{6,7,8}Li, ^{7,9,10}Be, ^{10,11}B, and C produced in collisions of 1.2, 1.9, and 2.5 GeV protons with a Ni target. The shape of the spectra and angular distributions almost does not change whereas the absolute value of the cross sections increases by a factor ∼1.7 for all ejectiles in this beam energy range. It was found that energy and angular dependencies of the cross sections cannot be reproduced by microscopic models of intranuclear cascade including coalescence of nucleons coupled to statistical model for evaporation of particles from excited, equilibrated residual nuclei. The inclusion of nonequilibrium processes, described by a phenomenological model of the emission from fast and hot moving sources, resulting from break up of the target nucleus, leads to very good reproduction of data. Cross sections of these processes are quite large, exhausting approximately half of the total production cross sections. Due to good reproduction of energy and angular dependencies of $d^2\sigma/d\Omega dE$ it was possible to determine total production cross sections for all studied ejectiles. Results obtained in this work point to the analogous reaction mechanism for proton induced reactions on Ni target as that observed previously for Au target in the same beam energy range.

DOI: 10.1103/PhysRevC.82.034605 PACS number(s): 25.40.Sc, 25.40.Ve

I. INTRODUCTION

The recent analysis [1,2] of the inclusive spectra and angular distributions of double differential cross sections $d^2\sigma/d\Omega dE$ for light charged particles (LCP's), i.e., particles with $Z \leqslant 2$, and intermediate mass fragments (IMF's), i.e., ejectiles heavier than ^{4}He, produced in proton-Au collisions at proton beam energies 1.2, 1.9, and 2.5 GeV indicated that the traditional picture of spallation reactions fails to describe the experimental data. This picture assumes that the reaction proceeds in two steps, namely as the intranuclear cascade of nucleon-nucleon interactions followed by evaporation of particles from an equilibrated residuum of the cascade. It was thus concluded that a significant contribution of other, presumably nonequilibrium, processes to the reaction mechanism is present.

It was found that the difference between the data and theoretical cross sections from the above two-step model varies smoothly with the scattering angle and with the energy of the ejectile. It turned out, that this variation may be well reproduced assuming the isotropic emission of nucleons and composite particles in the rest frame of two or three sources moving forward, i.e., along the beam direction. Such an effect has been interpreted in Refs. [1,2] as indication of a breakup of the target nucleus induced by the incident protons. In that physical picture the proton drills a cylindrical hole in the nucleus knocking out the small group of nucleons placed on the straight way of the proton through the nucleus. This group moves quickly in forward direction behaving as a fireball, which on its part emits nucleons and LCPs whereas the "wounded" nucleus may decay into two excited prefragments which also serve as sources of LCPs and IMFs.

Whereas the above interpretation of the observed effects is certainly not unique, the possibility to well reproduce the differential cross sections by means of a simple, phenomenological formula added to traditionally applied microscopic formalism opens several appealing opportunities: First, it enables to extract total production cross sections starting from measured double differential cross sections due to reliable interpolation and extrapolation of angular and energy dependencies of the data. Then, it allows to compare such total cross sections for different beam energies and different targets looking for systematic variation of the effects which cannot be reproduced by the traditional model of the spallation reactions. Knowledge of these systematic effects may give hints to development of new theoretical models and to verification of those which are at present available.

The present study was performed with the aim to investigate, whether the reaction mechanism observed and described in detail in Ref. [2] for Au target is also realized in collisions of protons with other target nuclei. The Ni target was used for this purpose because it has quite different properties than the Au target. The Ni nucleus is more than three times lighter, its N/Z ratio (∼1.1) is approximately 1.4 times smaller from that of the Au nucleus (N/Z ∼1.5), and its binding energy (∼8.8 MeV/nucleon) is significantly larger than that of the Au nucleus (∼7.9 MeV/nucleon). The appearance of the same reaction mechanism for such different target nuclei might

*Corresponding author: ufkamys@cyf-kr.edu.pl

suggest that this phenomenon is of a general character, i.e., it occurs for all target nuclei in the studied energy range.

To facilitate the comparison of the results from the present study of the reactions in the p + Ni system with results of previous investigations concerning the p + Au system [2], the present paper is organized in similar way as reference [2]. Experimental data are discussed in the next section, the theoretical analysis is described in the third section starting from IMF data and followed by analysis of LCPs cross sections, the discussion of results is presented in the fourth and the summary with conclusions in the fifth section.

II. EXPERIMENTAL DATA

The experiment was performed with the self-supporting Ni target of the thickness about of 150 μg/cm^2, irradiated by internal proton beam of COSY (COoler SYnchrotron) of the Jülich Research Center. The experimental setup and procedure of data taking were described in Refs. [1] and [3] in detail. The beam was operated in so called supercycle mode to assure identical experimental conditions for all three studied proton energies—1.2, 1.9, and 2.5 GeV, i.e., the same setup, electronics, the target thickness, and its position. In this mode several cycles were alternated for each requested beam energy, consisting of protons injection from JULIC cyclotron to COSY ring, their acceleration with the beam circulating in the ring below the target, and irradiating the target by slow movement of the beam in the upward direction. The using of supercycle mode minimizes systematic effects which might distort the studied energy dependence of the cross sections.

Double differential cross sections $d^2\sigma/d\Omega dE$ were measured at seven scattering angles; 16°, 20°, 35°, 50°, 65°, 80°, and 100° as a function of energy of ejectiles for the following isotopes ^{1,2,3}H, ^{3,4,6}He, ^{6,7,8}Li, ^{7,9,10}Be, and ^{10,11}B. The carbon ejectiles were only charge identified.

The absolute normalization of the cross sections was achieved by comparing the total production cross sections of ^{7}Be particles, obtained by angle and energy integration of measured differential cross sections, with values of ^{7}Be total production cross sections published in the compilation of Bubak *et al.* [4].

Such a method of normalization relies on proper interpolation and extrapolation of measured differential cross sections to energy and angular regions which were not studied in the experiment. To assure this the experimental energy spectra of ^{7}Be particles from the present experiment were fitted by a phenomenological formula of a single moving source, emitting isotropically these ejectiles. The detailed formulation of the model and interpretation of the parameters are given in Ref. [5] and in the Appendix of Ref. [1]. One of the parameters of the formula, i.e., σ is equal to angle and energy integrated $d^2\sigma/d\Omega dE$. Values of the parameters were searched for by simultaneous fit of the model predictions to the spectra measured at all scattering angles investigated in the present experiment. Very good description of all ^{7}Be spectra was achieved, assuring good interpolation of the data over energy and angle. The error of extrapolation of the data in the angular integration should be also negligibly small because of a smooth variation of the data with the angle. The main error of integration can appear due to inaccuracy in extrapolation of the $d\sigma/d\Omega dE$ to low, not measured energies of ^{7}Be, where the cross sections may achieve large values. The main factor influencing the total cross section is the height and position of the Coulomb barrier between the ^{7}Be ejectile and the residual nucleus. Information on the shape of the energy spectrum of ^{7}Be in the low energy region—close to the Coulomb barrier—was not available in the present study but could be found from experiments in which the inverse kinematics has been applied, i.e., when the hydrogen target was bombarded by heavy ions. In such an experiment all ejectiles have high enough energy in the laboratory system to be detected. Results of the recent experiment performed by CHARMS Collaboration at 1A GeV energy of ^{56}Fe beam on hydrogen target show that the experimental energy spectra of ^{6}Li, ^{12}C (cf. Fig.12 of Ref. [6]) as well as ^{7}Be and ^{9}Be [7] have Maxwellian shape with position of the maximum slightly below the simple estimation of the Coulomb barrier by the formula $Z_1Z_2/(A_1^{1/3} + A_2^{1/3})$ MeV, where Z_1,Z_2 and A_1,A_2 are the atomic and mass numbers of the ejectile and residual nucleus, respectively. The information on the shape of the spectra of ^{7}Be in the neighborhood of the Coulomb barrier put stringent constraints to the value of differential cross sections extrapolated to lowest energies. The spread of values of the σ parameter obtained in equivalent fits to the present ^{7}Be data, which were performed taking into consideration the above information on the shape of spectra, was smaller than 20%. Thus the absolute normalization of the present data was achieved by comparing the parameter σ of the above fits to the known experimental value of the total cross section for ^{7}Be production taken from the compilation of Bubak *et al.* [4].

A verification of the above procedure was performed in a twofold way: (i) The total production cross sections of all detected particles, extracted from analogous fits as that for ^{7}Be were compared with the total cross sections obtained by NESSI Collaboration for p + Ni collisions at proton beam energy 1.2 GeV in completely different experiment, in which an absolute normalization was obtained from monitoring all quantities influencing the magnitude of the cross sections [8]. It turned out that the present values of the total production cross sections at proton beam energy 1.2 GeV are in perfect agreement with total cross sections measured for all observed ejectiles. The ratio of the present cross sections to those of Herbach *et al.* [8] is shown in Fig. 1 (where the error of the ratio was calculated taking into account errors quoted in this reference as well as estimated errors of the present experiment). As can be seen the ratio of present cross sections and those from Ref. [8] is in the limits of errors equal to unity for all ejectiles. *This means that the normalization obtained due to analysis of ^{7}Be is appropriate for all ejectiles—it would be the same when extracted from analysis performed for other particles.*

(ii) The total cross sections for production of Li, Be, and B isotopes obtained in the present experiment from data normalized in the above manner at proton beam energy $T_p = 2.5$ GeV were compared to the total cross sections measured by Raisbeck *et al.* [9] also in p + Ni collisions but at

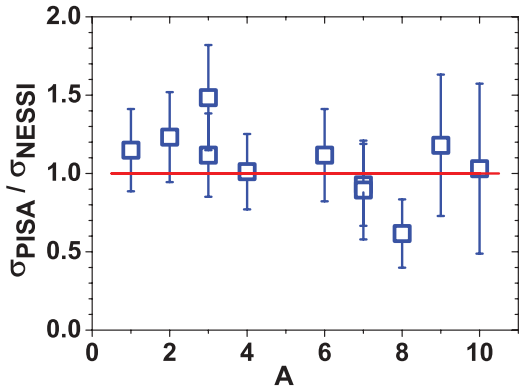

FIG. 1. (Color online) Ratio of the total production cross sections from the present experiment to those obtained in independent experiment of NESSI Collaboration [8] for p + Ni at $T_p = 1.2$ GeV.

$T_p = 3.0$ GeV. The same qualitative agreement of these data was observed as that for lower beam energy. This is illustrated by the upper panel of Fig. 2 where total production cross sections of the present work at 2.5 GeV are shown together with Li, Be, and B cross sections measured by Raisbeck *et al.* [9] on Ni target for 3.0 GeV proton beam. In the lower panel the comparison of present production cross sections to those obtained by the NESSI Collaboration is made at $T_p = 1.2$ GeV. The agreement is very good for both beam

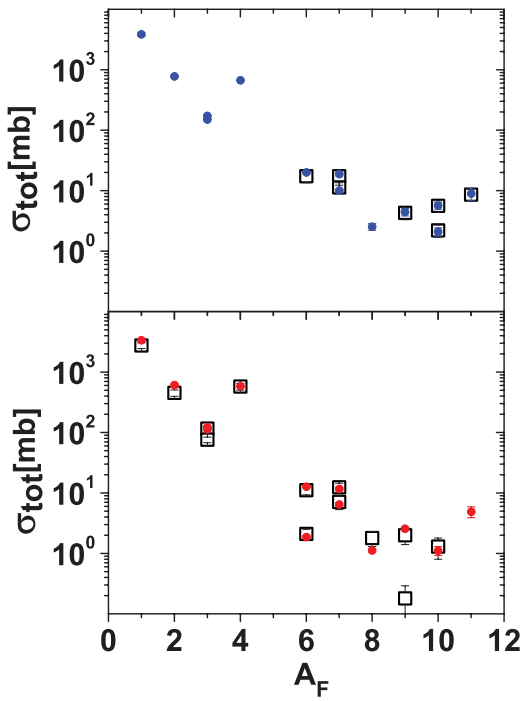

FIG. 2. (Color online) Upper panel: comparison of the total production cross sections from the present experiment on p + Ni collisions at $T_p = 2.5$ GeV (full dots) and those for Li, Be, and B ejectiles obtained by Raisbeck *et al.* [9] for the same nuclear system but at $T_p = 3.0$ GeV (open squares). Lower panel: the data from present experiment at $T_p = 1.2$ GeV (full dots) and total production cross sections measured by NESSI Collaboration [8] at the same energy (open squares).

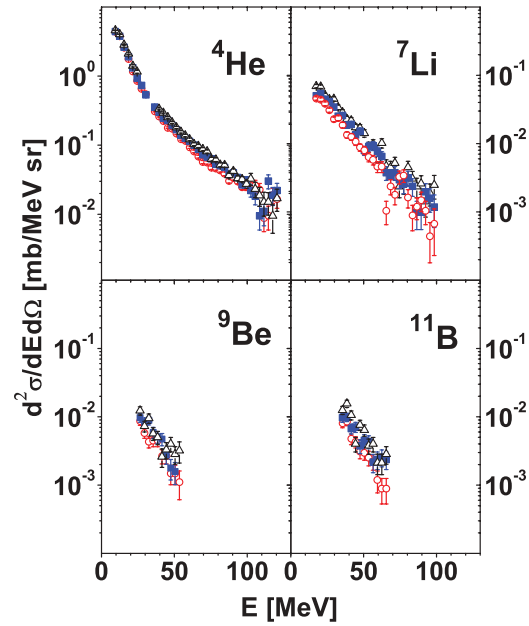

FIG. 3. (Color online) Typical spectra of ^{4}He, ^{7}Li, ^{9}Be, and ^{11}B ejectiles (upper left, upper right, lower left, and lower right parts of the figure, respectively) measured at 35° for three energies of the proton beam; 1.2, 1.9, and 2.5 GeV, impinging on to the Ni target. Open circles represent the lowest energy, full squares—the intermediate energy, and the open triangles show the data for the highest energy.

energies (the symbols representing different experiments are hardly distinguishable) *which means that the used method of normalization is exact enough to reproduce the energy dependence of the magnitude of cross sections.*

Typical spectra of isotopically identified ejectiles obtained in the present experiment are shown in Fig. 3. All spectra are smooth and do not change their shapes with increasing beam energy, however, the magnitude of the cross sections increases slightly with the energy.

III. THEORETICAL ANALYSIS

The analysis of the present experimental data was performed according to the same procedure as that applied previously to the data for proton induced reactions on the Au target in the work of Budzanowski *et al.* [2]. First, the cross sections were evaluated from the intranuclear cascade with inclusion of possibility to coalesce the outgoing nucleons into LCPs, and with possibility to evaporate the particles from excited, equilibrated residua of intranuclear cascade. Such two-step model of the reaction mechanism is most frequently used in the literature for the description of spallation reactions at high proton energies. The INCL4.3 computer program of Boudard *et al.* [10] has been used for calculations of the intranuclear cascade and the GEM2 program of Furihata [11,12] has been applied to evaluate evaporation cross sections. Since the data were generally underestimated by the two-step model a phenomenological analysis was performed in the following. This analysis was based on the assumption that additional processes exist besides the mechanisms described above.

They were parametrized by an incoherent sum of isotropic emission of particles from highly excited sources moving in forward direction, i.e., along to the beam direction. Each of the sources has a Maxwellian distribution of the energy E available for the two body decay resulting in emission of the detected particles; $d^2\sigma/dEd\Omega \sim \sqrt{E}\exp(-E/T)$. The velocity of the source—β (in units of speed of light), its temperature—T (in MeV), and the contribution to the total production cross section—σ are treated as free parameters. The presence of the Coulomb barrier, which hinders emission of low energy particles, was taken into account multiplying the Maxwellian energy distribution by a smooth function $P(E)$ corresponding to the transmission probability through the barrier. Two parameters were introduced to characterize the properties of the Coulomb barrier: k parameter, i.e., height of the Coulomb barrier in units of the height of the barrier B of two charged, touching spheres of radius $1.44A^{1/3}$; $B = Z_1Z_2e^2/1.44(A_1^{1/3} + A_2^{1/3})$ MeV, and the ratio B/d, where d is the diffuseness of the transmission function through the barrier: $P(E) = \{1 + \exp[(E - kB)/d]\}^{-1}$. Details of this procedure, as well as the interpretation of parameters of the model can be found in the Appendix of Ref. [1].

A. Intermediate mass fragments

The shape of the spectra of IMFs is almost independent of the beam energy. Thus, only the cross sections measured at 2.5 GeV beam energy have been used for illustration of the quality of data description. On the contrary, the shape of the spectra changes in a regular way with the variation of the detection angle, namely the spectra become more steep when the scattering angle increases. This is especially well visible when the data are compared at angles differing strongly as, e.g., 35° and 100°. Experimental spectra measured at three selected angles—35°, 80°, and 100°—are shown on Fig. 4 for most abundant isotopes of lithium, beryllium, and boron as open circles together with the evaporation model predictions (solid lines). Fluctuations of the theoretical spectra are due to the Monte Carlo method of model calculations, i.e., due to limited statistics of generated events. As can be seen, the theoretical spectra are more steep than the experimental ones and the absolute values of theoretical cross sections are several times smaller than the data. The former effect is most pronounced for ^{6,7}Li and ^{7}Be cross sections whereas the latter is present for all detected IMFs. Furthermore, the evaporation model does not reproduce the tendency of the shape variation with the angle.

All these facts indicate that an important contribution of another reaction mechanism must be added to the evaporation cross sections to assure a good reproduction of the data. This contribution is comparable in magnitude with the evaporation cross section for Li and becomes even more dominant for Be and B isotopes. Thus, the IMF data have been analyzed in the frame of a phenomenological model of two moving sources as it was done for p + Au reactions [1]. In this way the IMF production on Ni target could be compared with that for the Au target.

The parameters of two moving sources were searched for by fitting the two moving sources cross sections to experimental

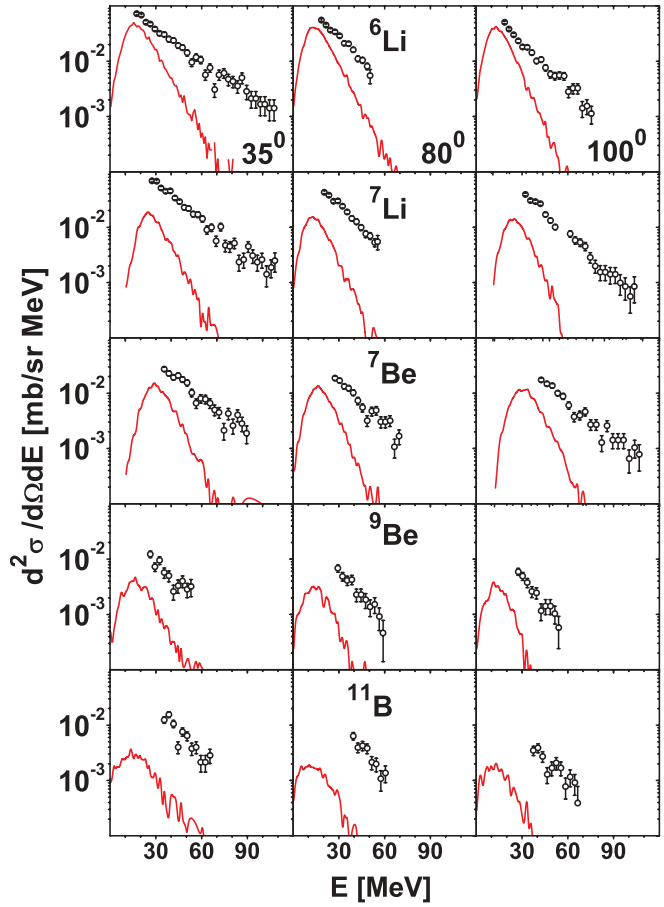

FIG. 4. (Color online) Typical spectra of selected lithium, beryllium, and boron isotopes from p + Ni collisions measured at 35°, 80°, and 100° (left, middle, and right columns, respectively) for 2.5 GeV proton beam impinging on to the Ni target. The detected particles are listed in the central panel of each row of pictures. Open circles represent the experimental data, and solid lines correspond to intranuclear cascade followed by evaporation of particles, respectively.

data, which consisted of energy spectra measured at seven angles: 16°, 20°, 35°, 50°, 65°, 80°, and 100°. To decrease the number of parameters it was assumed that the velocity of the slow source emitting IMF's is equal to the velocity of the heavy residuum from intranuclear cascade, i.e., $\beta_1 = 0.005$. The mean values of this velocity was found in calculations of intranuclear cascade to be equal to $0.0051c$, $0.0049c$, and $0.0047c$ for 1.2, 1.9, and 2.5 GeV beam energy, respectively. It was checked that the modification of this parameter by 30% causes changes of other parameters smaller than their errors estimated by fitting computer program. In evaluation of k parameter it was assumed that B value is defined as the Coulomb barrier between the emitted particles and the target nucleus. The results of the fit are not very sensitive to the value of the k parameter because the experimental low energy limit of the spectra is above the position of the Coulomb barrier for most of IMFs. Thus fixed values of $k_1 = 0.75$ and $k_2 = 0.3$ were used. The B/d ratio was arbitrarily assumed to be equal to 5.5.

TABLE I. Parameters of two moving sources fitted to p + Ni data for isotopically identified IMFs and for ^{4}He: β_i, T_i, and σ_i correspond to source velocity, its apparent temperature, and total production cross section, respectively. The sum $\sigma \equiv \sigma_1 + \sigma_2$ is also listed. The left part of the table (parameters with indices "1") corresponds to the slow moving source, and the right part contains values of parameters for the fast moving source. The upper row for each ejectile corresponds to beam energy 1.2 GeV, the row in the middle to 1.9 GeV, and the lowest one to the energy 2.5 GeV.

Ejectile	Slow source		Fast source			σ	χ^2
	T_1/MeV	σ_1/mb	β_2	T_2/MeV	σ_2/mb	mb	
^{4}He	7.0(2)	244(6)	0.040(3)	18.1(5)	76(6)	320(9)	7.3
	7.3(2)	269(6)	0.036(2)	19.4(5)	94(6)	363(9)	4.7
	7.9(2)	283(8)	0.035(2)	20.1(5)	101(7)	384(11)	4.4
^{6}Li	9.1(4)	8.3(4)	0.035(3)	18.6(5)	4.1(5)	12.4(7)	1.5
	10.4(4)	11.5(6)	0.037(3)	19.8(5)	4.5(6)	16.0(9)	1.4
	9.4(5)	11.6(8)	0.026(3)	20.5(6)	8.0(9)	19.6(1.2)	1.3
^{7}Li	8.1(7)	4.9(7)	0.022(2)	14.7(4)	6.6(9)	11.5(1.2)	1.3
	9.6(7)	8.0(1.0)	0.025(3)	15.9(5)	7.0(1.2)	15.0(1.6)	1.3
	9.6(1.0)	5.2(1.3)	0.018(2)	16.0(5)	12.3(1.8)	17.5(2.2)	1.4
^{8}Li	[8.0]	[0.2]	0.040(8)	14.4(2.0)	1.2(5)	1.4(5)	1.4
	9.4(3.8)	0.6(5)	0.032(6)	17.2(1.1)	3.7(1.0)	4.3(1.1)	1.0
	8.0(1.8)	1.3(4)	0.029(5)	18.0(1.0)	6.4(1.5)	7.7(1.6)	1.0
^{7}Be	8.7(1.3)	2.8(5)	0.025(3)	16.8(7)	3.6(7)	6.4(9)	1.4
	9.5(9)	4.9(6)	0.025(3)	19.2(9)	3.9(8)	8.8(1.0)	1.0
	11.3(7)	6.9(6)	0.032(5)	21.4(1.3)	2.6(7)	9.5(9)	1.0
^{9}Be	[8.6]	1.1(2)	[0.023]	12.1(8)	1.3(2)	2.4(3)	1.1
	8.1(1.6)	2.0(5)	0.024(7)	14.2(1.2)	1.6(7)	3.6(9)	0.8
	8.3(2.0)	2.4(7)	0.019(7)	16.9(2.4)	1.8(1.1)	4.2(1.3)	1.0
^{10}Be	6.1(1.9)	1.0(4)	0.030(16)	27.8(9.0)	0.4(2)	1.4(5)	1.8
	7.9(1.7)	1.0(4)	[0.023]	17.6(3.1)	0.7(2)	1.7(5)	1.8
	6.1(1.9)	1.7(6)	0.024(11)	23.0(9)	0.8(4)	2.5(7)	1.3
^{10}B	[6.0]	1.6(1.2)	0.018(4)	15.5(3.1)	1.7(6)	3.3(1.4)	1.7
	[6.0]	3.3(1.2)	[0.023]	16.4(1.5)	2.4(4)	5.7(1.3)	1.8
	[6.0]	3.2(1.4)	[0.023]	17.7(1.8)	2.7(4)	5.9(1.5)	1.9
^{11}B	[6.0]	3.1(9)	[0.023]	13.4(1.2)	1.8(3)	4.9(1.0)	1.3
	[6.0]	5.2(1.2)	[0.023]	17.8(2.2)	2.3(3)	7.5(1.3)	1.5
	[6.0]	5.9(3.6)	0.016(4)	14.8(3.2)	4.1(1.8)	10(4)	1.7

Values of the best fit parameters are listed in Table I. The errors of the parameters are also given when the program searching for the best fit could estimate them. However, sometimes the program was not able to estimate the errors, especially when strong ambiguities of parameters were present. In such a case the values of the parameters are quoted without estimation of errors. Sometimes it was useful to fix the values of parameters to avoid numerical problems leading to ambiguities. Such values are quoted in the table in parentheses.

A very good description of the spectra of all IMF's has been obtained as can be judged from the inspection of Fig. 5 and values of the χ^2 given in the Table I, which usually vary between 1 and 2.

It is obvious from comparison of Figs. 4 and 5 that the spectra of particles emitted from the slow source are very similar to the evaporation spectra of particles from the residuum of intranuclear cascade, however, it is not the case for the spectra of the fast source. They have much smaller slope and are dependent on the scattering angle. It is evident that their presence is necessary to reproduce the high energy part of experimental spectra.

The cross sections of both emitting sources increase with beam energy. This is illustrated in Fig. 6 where the ratios of the production cross sections for beam energy 1.2 and 1.9 GeV to the cross sections for 2.5 GeV are presented. The cross sections increase approximately by factor 1.7 when beam energy increases from 1.2 GeV to 2.5 GeV (cf. numbers depicted in Fig. 6). Since the energy dependence is very similar for both emitting sources, the relative contributions of the sources remain constant in the studied energy range and, moreover, both are equal in the limits of errors: The averaged over IMFs ratio of $\sigma_2/(\sigma_1 + \sigma_2)$ is equal to 0.50(14), 0.46(11), and 0.48(16) for beam energies 1.2, 1.9, and 2.5 GeV, respectively. Thus, this ratio averaged over three energies is equal to 0.48(7).

The parameters of the sources, which influence the shape of the spectra (velocity β and temperature T) should not change with the beam energy because the shape of experimental spectra is independent of the beam energy (cf. Fig. 3).

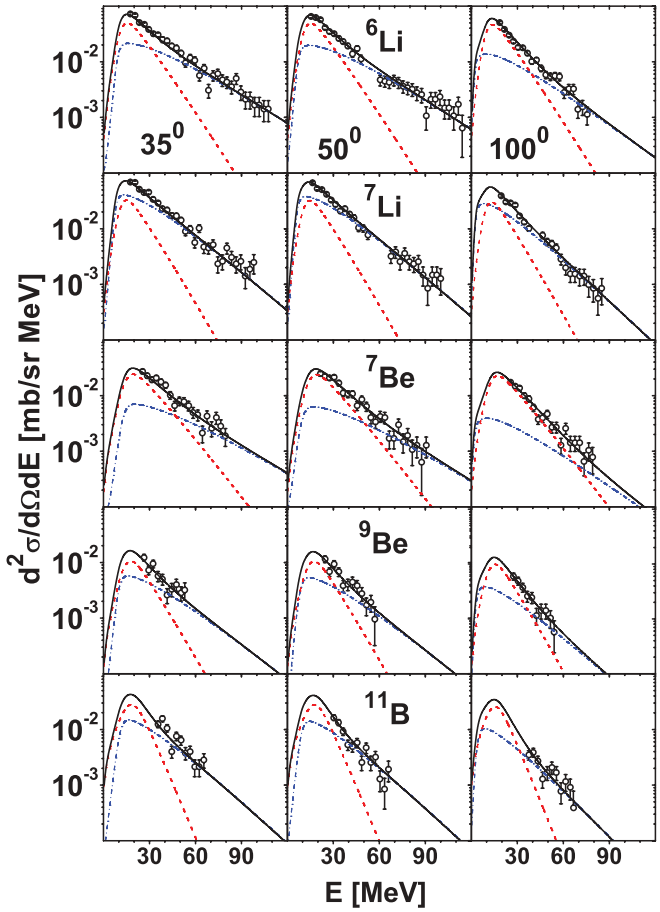

FIG. 5. (Color online) Typical spectra of lithium, beryllium, and boron ejectiles from p + Ni collisions measured at 35°, 50°, and 100° (left, middle, and right columns, respectively) for 2.5 GeV proton beam impinging on to the Ni target. The detected particles are listed in the central panel of each row of pictures. Open circles represent the experimental data, dashed, dot-dashed, and solid lines correspond to slow emitting source, fast emitting source and the sum of both contributions, respectively.

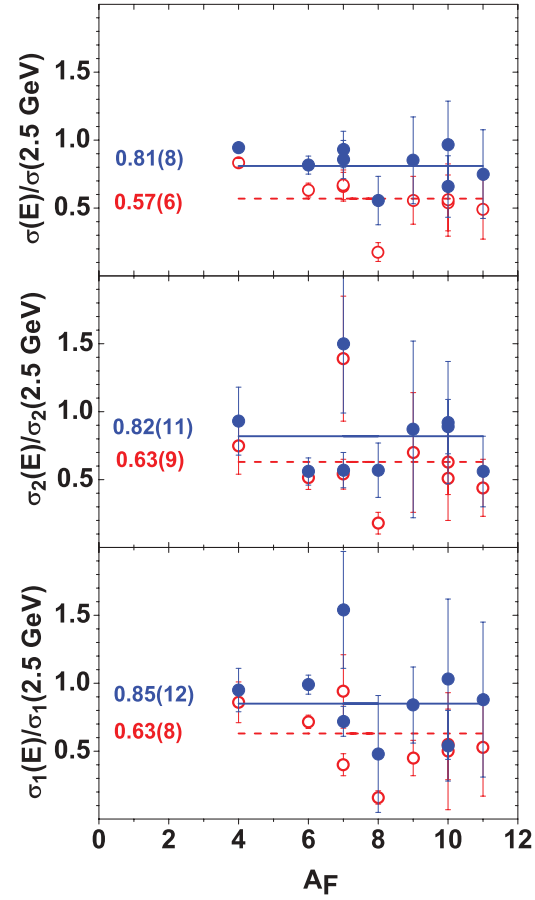

FIG. 6. (Color online) Ratio of production cross section determined at 1.2 (open circles) and 1.9 GeV (full dots) to the cross sections found at 2.5 GeV beam energy. The lower panel presents cross sections for slow sources, panel in the middle for fast sources, and upper panel for sum of both contributions. The horizontal lines depict values of the ratios averaged over IMFs; the solid lines for the 1.9 GeV and the dashed lines for 1.2 GeV.

However, there is a distinct difference for each energy between values of the parameters characterizing the slow source and the fast source. The velocity of the fast source β_2, averaged over IMFs is equal to 0.027(3), 0.027(2), and 0.023(2) for beam energy 1.2, 1.9, and 2.5 GeV, respectively. These values are about five times larger than fixed velocity of the slow source ($\beta_1 = 0.005$). The temperature parameter T_2 of the fast source is about two times larger than the temperature parameter of the slow source T_1. Its values (averaged over IMFs) are equal to 16.8(1.2), 17.4(6), and 17.8(8) MeV for the fast source and 7.6(3), 8.4(6), and 8.1(5) MeV for the slow source at three studied beam energies 1.2, 1.9, and 2.5 GeV, respectively.

B. Light charged particles

All experimental spectra of LCPs from p + Ni collisions contain large high energy component (cf. Figs. 3, 7, and 8), which cannot be reproduced by evaporation of particles from the equilibrated remnant of the intranuclear cascade. Thus, the nonequilibrium emission of LCPs must play an important role. The coalescence of nucleons escaping from the target nucleus together with nucleons taking part in the intranuclear cascade may lead to such an emission. Indeed, Boudard *et al.* [10] and Letourneau *et al.* [13] have shown that the microscopic calculation of coalescence occurring when the intranuclear cascade proceeds is able to reproduce a large part of high energy tails of the spectra. However, it was found that the improvement of the description of LCPs spectra deteriorates simultaneously the proton spectra because increasing of the production of composite particles occurs on the account of decreasing emission of the nucleons. This contradiction led the present authors to search for another nonequilibrium process, which could be responsible for the observed enhancement of the high energy part of the LCP spectra. It was proposed [2], that the emission from a fireball, i.e., a fast and hot group of nucleons consisting of target nucleons lying on the straight way of the bombarding proton through the target nucleus [14], can account for the missing nonequilibrium component of the LCP cross sections. A sum of the coalescence of nucleons and

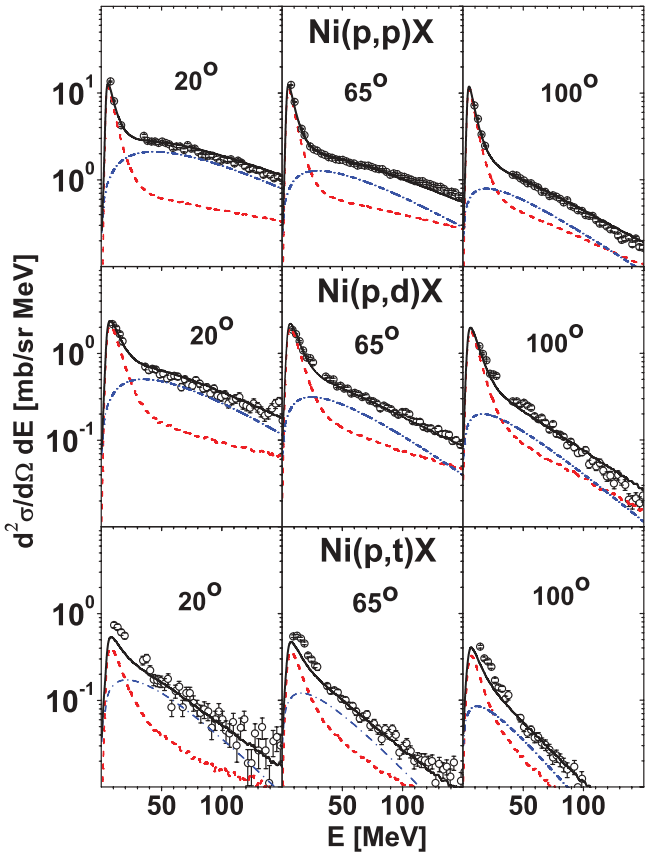

FIG. 7. (Color online) Typical spectra of protons, deuterons, and tritons (upper, middle, and lower rows of the figure, respectively) measured at 20°, 65°, and 100° (left, middle, and right columns of the figure, respectively) for 2.5 GeV proton beam impinging on to the Ni target. Open circles represent the experimental data, dashed, dot-dashed, and solid lines correspond to the two-step model, the emission from the fireball and the sum of both contributions, respectively.

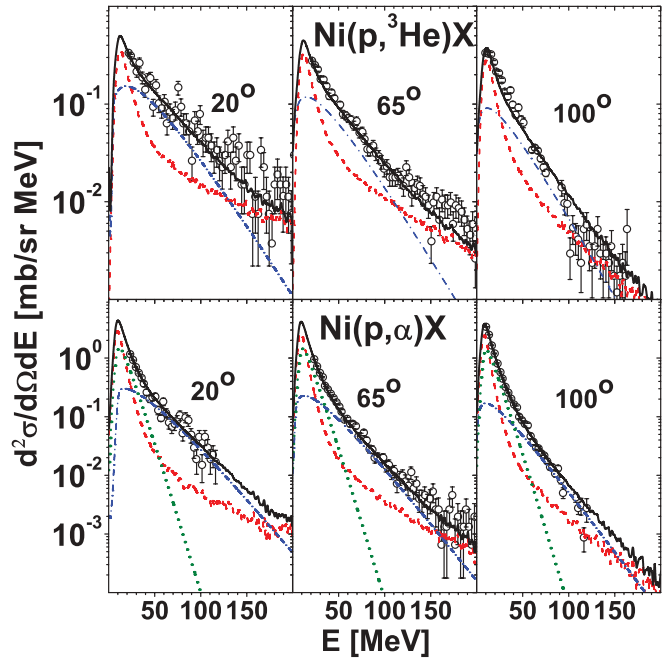

FIG. 8. (Color online) Same as on Fig. 7 but for ^{3}He and ^{4}He. The dotted line for ^{4}He denotes the contribution of an additional, slowly moving source.

the emission of LCPs from the fireball was found to be crucial for the very good description of the data for proton induced reactions on Au target at three beam energies: 1.2, 1.9, and 2.5 GeV [2]. Furthermore, the emission of the fireball, which introduces a strong rearrangement of the target nucleus can lead to a breakup of the remnant of the target and thus to an appearing of two moving sources also emitting intermediate mass fragments and LCPs. Therefore, this hypothesis explains simultaneously the presence of the nonequilibrium emission for IMFs which was discussed above.

Since the fireball contains only several nucleons its contribution is present only for LCPs. On the contrary, the fast and slow excited prefragments of the target may emit IMFs as well as LCPs. In the present analysis their contribution to spectra of LCPs has been, however, neglected because it was estimated (by extrapolation of parameters found for IMFs to lighter ejectiles) to be much smaller than contributions of other reaction mechanisms. The magnitude of cross sections for the emission of LCPs from two sources—products of breakup—was estimated to be ∼10% of the total cross sections, i.e., to be of order of errors of the fitting procedure.

In the present study the same procedure of the description of LCP spectra as that in Ref. [2] has been applied. The INCL4.3 computer program [10] has been used for the description of the intranuclear cascade of nucleon-nucleon collisions with inclusion of coalescence of nucleons, whereas the GEM2 computer program [11,12] served for the evaluation of evaporation of particles from heavy target residua remaining after the intranuclear cascade. The default parameter values, proposed by the authors of both programs, have been used, respectively.

Since there is no explicit room for the presence of the fireball in the microscopic calculations performed according to the intranuclear cascade model, the inclusion of fireball emission should be accompanied by decreasing the contribution from direct processes simulated by intranuclear cascade and coalescence of escaping nucleons. Thus, the spectra of protons evaluated from intranuclear cascade with inclusion of coalescence and with a contribution of the evaporation of particles were multiplied by a factor F, common for all scattering angles, treated as a free parameter and then added to the contribution from the fireball emission calculated according to the formula of single moving source emitting isotropically the LCPs [5]. The same, fixed value of the scaling factor has been used for further analysis of data for other LCPs. The parameters of the single moving source, the fireball, i.e., its temperature parameter—T_3, velocity of the source—β_3, total production cross section associated with this mechanism—σ_3, were treated also as free parameters.

Parameters k_3 (the height of the Coulomb barriers in units of B, Coulomb barrier between the ejectile and the target nucleus) and parameter B/d describing the diffuseness of the transmission function through the Coulomb barrier are fixed

TABLE II. Parameters of the fireball fitted to p + Ni data; β_3, T_3, and σ_3 correspond to the fireball velocity in units of speed of light, its apparent temperature, and total production cross section, respectively. The upper row for each ejectile corresponds to beam energy 1.2 GeV, the row in the middle to 1.9 GeV, and the lowest one to the energy 2.5 GeV. The parameter F is the scaling factor of the coalescence and evaporation contribution extracted from a fit to the proton spectra. The numbers in parentheses show fixed values of the parameters. Note, that for the α particle contribution of two additional moving sources should be added with parameters given in Table I. The columns described as $F * \sigma_{INCL}$ and $F * \sigma_{GEM}$ contain total production cross sections due to the intranuclear cascade with the coalescence and due to evaporation from the target residuum, respectively. The total production cross section obtained by summing of all contributions is depicted in the column denoted by σ. In the case of alpha particles it contains also the contribution of the emission from slow and fast sources listed in Table I.

Ejectile	β_3	T_3 MeV	σ_3 mb	F	$F * \sigma_{INCL}$ mb	$F * \sigma_{GEM}$ mb	σ mb	χ^2
p	0.149(12)	38.9(2.1)	1071(61)	0.70(3)	1094	994	3159(61)	179
	0.156(10)	41.7(1.9)	1222(53)	0.70(2)	1139	1005	3366(53)	95.1
	0.163(8)	43.2(1.5)	1343(44)	0.79(2)	1286	1123	3752(44)	48.8
d	0.105(4)	32.5(8)	181(5)	[0.70]	202	174	557(5)	9.5
	0.099(3)	33.7(6)	234(5)	[0.70]	201	196	631(5)	3.2
	0.100(4)	35.8(8)	272(7)	[0.79]	220	225	717(7)	7.4
t	0.062(3)	21.9(6)	41.9(1.6)	[0.70]	40.9	28.9	111.7(1.6)	1.3
	0.055(3)	23.8(6)	59.8(2.1)	[0.70]	41.3	34.1	135.2(2.1)	1.4
	0.054(3)	25.0(6)	71.5(2.2)	[0.79]	45.3	39.4	156.2(2.2)	1.3
^{3}He	0.046(2)	22.9(5)	43.1(1)	[0.70]	31.2	32.6	106.6(1)	3.4
	0.039(2)	23.5(4)	60.5(1.2)	[0.70]	31.6	37.5	129.6(1.2)	3.3
	0.040(2)	25.0(5)	69.4(1.4)	[0.79]	34.5	43.1	147.0(1.4)	2.9
^{4}He				[0.70]	16.8	277	614(9)	7.3
				[0.70]	16.6	281	661(9)	4.7
				[0.79]	18.1	312	714(11)	4.4

at arbitrarily assumed values 0.07 and 4.8, respectively. Values of the fitted parameters are collected in Table II.

The fit was performed for seven scattering angles (16°, 20°, 35°, 50°, 65°, 80°, and 100°). Results of the fit are presented in Fig. 7 for protons, deuterons and tritons, and in Fig. 8 for ^{3}He and ^{4}He. Since the spectra at various beam energies do almost not differ in the shape, the comparison of theoretical cross sections with the data is shown only for one beam energy, namely for 2.5 GeV. The left column on both figures represents cross sections for 20°, the column in the middle for 65°, and the right column the data measured at 100°. The proton spectra are shown in the upper row of Fig. 7, the deuteron and triton data in the middle and lower row, respectively. The ^{3}He data are depicted in the upper row of Fig. 8, whereas the ^{4}He cross sections occupy the lower row of this figure.

It is obvious from inspection of Figs. 7 and 8, that a very good description of the experimental data for all LCPs was achieved. It should be emphasized, that the values of the best fit parameters vary smoothly from ejectile to ejectile as well as from the one beam energy to another, thus the same mechanism seems to be responsible for the nonequilibrium processes for all these particles. It was, however, found that values of the parameters, necessary to describe the α particle data differ from those for lighter LCPs. It turned out that (i) it is necessary to use two emitting sources instead one fireball for good data reproduction, and (ii) the parameters of these sources have quite similar values as those for IMFs (cf. Table I). For this reason, it may be concluded that the α particles behave rather like IMFs than as LCPs.

Values of fireball velocity β_3 and its temperature parameter T_3 do not change systematically with the beam energy and their fluctuations are so small, that it is possible to assume that they do not change with the energy. A similar situation was observed for IMFs. Thus the energy averaged values of velocities and temperature parameters of all sources are collected in one figure—Fig. 9—to allow for discussion of their dependence on the mass of ejectiles.

The velocities and temperature parameters are grouped in three distinctly separated sets corresponding to the slow source (β_1 and T_1), to the fast source (β_2 and T_2), and to the fireball (β_3 and T_3). The mass dependence—approximated by straight lines—is also different for each source. The slope of the mass dependence is the smallest for the slow source, of intermediate value for the fast source, and the largest for the fireball. A linear dependence of the temperature parameter on the mass of ejectiles is expected as a result of momentum conservation, i.e., the recoil of the source of a given mass appears during the emission of ejectiles of various masses. This linear dependence of the temperature parameter on the mass of ejectile allows for the extraction of recoil corrected temperature of the source τ and the estimation of the mass of the source A_S. If the mass of the source is constant—the same for all ejectiles—the determination of its mass and recoil corrected temperature is unambiguous. However, there are arguments that the source must have some distribution of masses with different average value for each ejectile. For example, the deuterons cannot be emitted by fireball consisted of only two nucleons but such emission may occur from the fireball built of three nucleons. The emission of protons, on the contrary, can appear both from

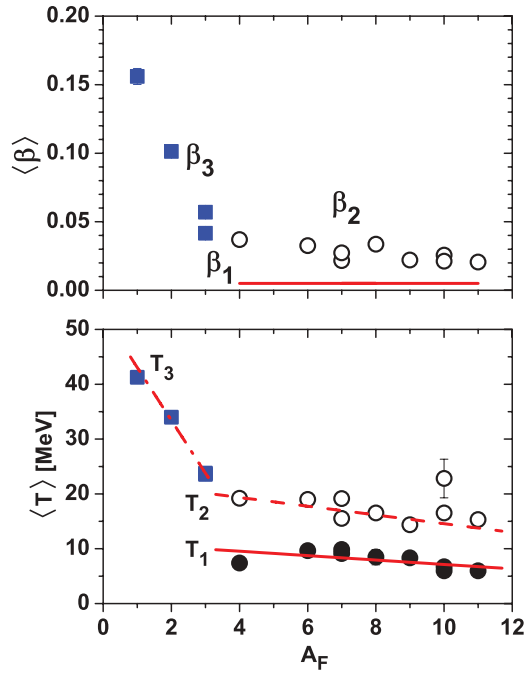

FIG. 9. (Color online) In the lower panel of the figure the apparent temperature of the moving sources, averaged over beam energies is drawn as a function of the ejectile mass. Open circles and full dots represent values of temperature parameters T_2 and T_1 for fast and slow source, respectively. Full squares indicate temperature T_3 of the fireball. The solid and dashed lines were fitted to the points representing the IMF's and ^{4}He. The dash-dotted line was fitted to points representing the LCP's. In the upper panel the dependence of the beam energy averaged velocity of the sources is drawn versus the mass of ejectiles. The symbols and lines have the same meaning as for the lower part of the figure with one exception: The full dots are not shown because the velocity of the slower source was fixed during the analysis (at velocity $\beta_1 = 0.005$ of heavy residuum of target nucleus after intranuclear cascade) and it is represented by a solid line.

two-nucleon and three-nucleon sources, thus the mass of the fireball emitting protons is in average smaller than the mass of fireball emitting the deuterons. This may be a reason of strong decreasing of the fireball velocity with the mass of the ejectile as well as only slight decreasing of the velocity of the fast source with the mass of IMFs. A change of the mass of the fireball by one nucleon is very significant, because the fireball may be built of only several nucleons, whereas such a change for the source consisted of 20 or more nucleons is hardly to be observed in the mass dependence of the temperature parameter.

The above given arguments show that the extraction of the mass of the source and its recoil corrected temperature from the ejectile mass dependence of the temperature parameter should be taken with caution and treated only as a crude estimation. Such an estimation is discussed below and extracted parameters are compared with those, which were found in our previous study [2] of reactions induced by protons on the gold target.

IV. DISCUSSION

The parameters of linear functions describing the dependence on the ejectile mass of the temperature parameter T and velocity β of three sources are collected in Table III. Those parameters, obtained in the previous study of reactions induced by protons on the gold target [2], are also listed in this table.

TABLE III. Beam energy averaged temperature and velocity parameters of three sources of ejectiles for Au and Ni targets. T denotes apparent source temperature (in MeV), τ is the temperature parameter corrected for the recoil, A_S represents mass number of the source, and β its velocity in units of speed of light. The symbol A indicates the mass number of the ejectile. Parameters with index 1 correspond to slow source, with index 2 to fast source, and with index 3 to the fireball.

Parameter	Au	Ni
T_1	11.1(3)	$11.2(7) - 0.4(2)*A$
τ_1	11.1(3)	11.2(7)
A_{S_1}	∼165	28(15)
β_1	[0.003]	[0.005]
T_2	$30.6(4) - 1.61(45)*A$	$22.5(6) - 0.8(1)*A$
τ_2	30.6(4)	22.5(6)
A_{S_2}	19(6)	28(4)
β_2	$0.059(5) - 0.0034(6)*A$	$0.044(6) - 0.0021(7)*A$
T_3	$49.9(7) - 8.2(2.6)*A$	$52.7(1.1) - 9.6(4)*A$
τ_3	49.9(7)	52.7(1.1)
A_{S_3}	6(2)	5.5(3)
β_3	$0.218(39) - 0.051(16)*A$	$0.209(11) - 0.053(5)*A$

It is clearly visible that *all properties of the fireballs for both targets are identical in the limits of errors*. This seems to be unexpected, especially as concerns masses of both fireballs, because of large difference between the mass of Ni and Au targets. However, according to the simple picture of the fireball, it is consisted of the nucleons which lie on its straight way through the target nucleus, therefore the mass of the fireball should scale as $A^{1/3}$. It means that the ratio of fireball masses for Au and Ni should be equal to ∼1.5. This ratio, extracted from the phenomenological analysis, is equal to 1.1(7) what means, that in the limits of errors it is in agreement with the assumed picture of the mechanism.

The equality of velocities of fireballs and their temperatures for both targets may be treated as consequence of the same momentum and energy transfer from the bombarding proton to the group of nucleons forming the fireball. Such an explanation is in line with the fact of the same beam energies for both targets and small difference in the thickness of the nuclear matter placed on the way of bombarding proton. Therefore, this equality may be interpreted as the argument in favor of assumed model of the reaction.

The recoil corrected temperatures of slow sources for Ni and Au targets are also the same. Of course, the mass A_{S_2} of the slow source is completely different in the case of Au target (∼165) and Ni target (∼28). Therefore the recoil correction of the temperature parameter could be neglected for the Au target but is visible in the ejectile mass dependence of the temperature parameter T_1 for the Ni target. This difference of source masses reflects also on the velocity of the slow source β_1.

The largest differences appear for the fast source. It should be, however, pointed out that the parameters do not differ

TABLE IV. Averaged over IMFs ratio of cross section σ_i for energy E to the same cross section measured at proton beam energy 2.5 GeV on Au and Ni targets. The σ_i is equal to σ_1 (slow source), σ_2 (fast source) or $\sigma \equiv \sigma_1 + \sigma_2$ (total production cross section)

Ratio of σ_i to σ_i(2.5 GeV)	at E/GeV	Au	Ni
σ_1	1.2	0.39(3)	0.63(8)
	1.9	0.75(6)	0.85(12)
σ_2	1.2	0.23(3)	0.63(9)
	1.9	0.57(6)	0.82(11)
$\sigma_1 + \sigma_2$	1.2	0.33(2)	0.57(6)
	1.9	0.66(4)	0.81(8)

in average more than ∼50%. Taking into consideration the accuracy of extraction of values of the parameters it may be claimed that the parameters of the fast source are similar for both targets.

The above considerations concern *velocity and temperature of three sources for Au and Ni targets* and show, that these parameters, which are almost independent of the beam energy in the studied proton energy range 1.2–2.5 GeV, *are very similar for both targets.*

In the following the behavior of production cross sections will be discussed. As it was shown in Fig. 6, cross sections for all IMFs increase on average by factor ∼1.7 when proton beam energy increases from 1.2 GeV to 2.5 GeV. This is true for the total production cross sections as well as for the contributions of individual emitting sources, however, the spread (among various IMFs) of the ratio of given cross section to that measured at 2.5 GeV is smaller for total production cross section than for individual sources. The ratios of the cross sections measured at 1.2 and 1.9 GeV to those measured at 2.5 GeV are listed in Table IV.

It is clear from an examination of Table IV that the IMF production cross sections measured for Au target increase

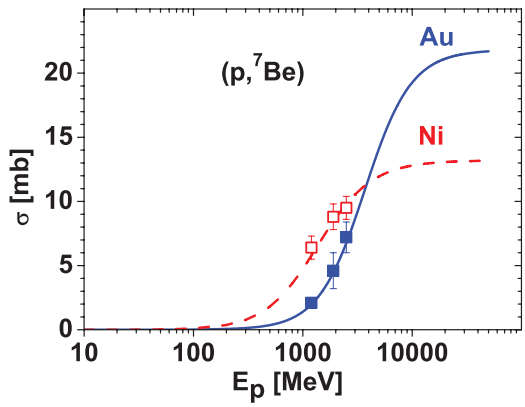

FIG. 10. (Color online) Energy dependence of the production cross section of ^{7}Be ejectiles in proton induced reactions. The lines show results of a compilation of ^{7}Be production cross sections [4], the symbols represent experimental data of the present experiment (open squares) for a Ni target and the data published by Budzanowski *et al.* [2] (full squares) for an Au target. The solid and dashed lines depict the excitation functions from Ref. [4] for Au and Ni targets, respectively.

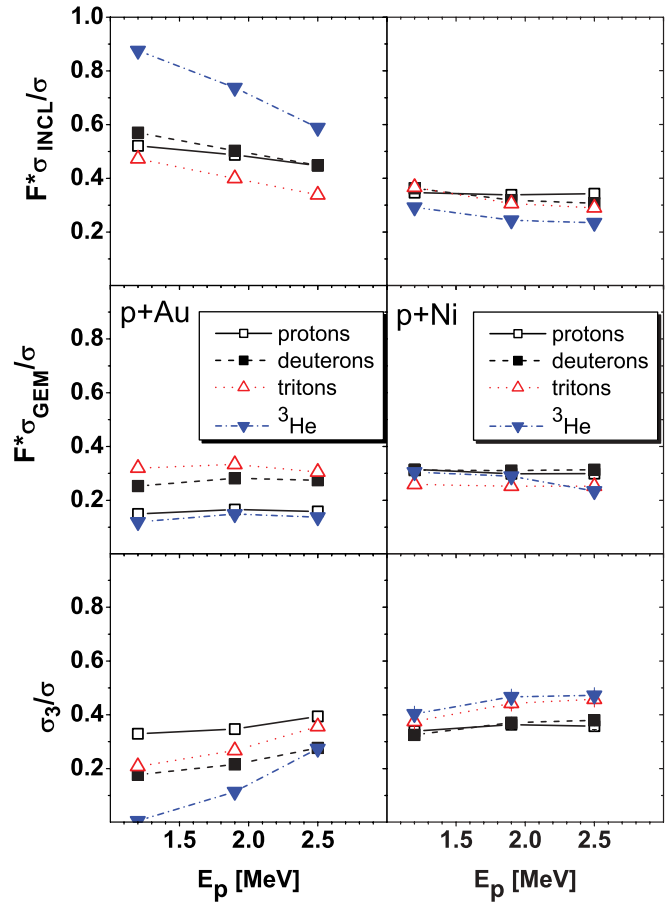

FIG. 11. (Color online) Energy dependence of various reaction mechanisms for protons (open squares), deuterons (full squares), tritons (open triangles), and ^{3}He (full triangles). The relative contribution of the fast stage of the reaction, i.e., intranuclear cascade and coalescence of nucleons into LCPs σ_{INCL}/σ is presented in the upper panel of the figure, evaporation contribution from the equilibrated residuum of the intranuclear cascade σ_{GEM}/σ is shown in the middle panel, whereas the contribution of fireball emission σ_3/σ is depicted in the lower panel.

stronger with beam energy than those for Ni target. This can be understood as an effect caused by difference between threshold energies for fragmentation of both targets. To illustrate this effect the excitation function for ^{7}Be production is shown in Fig. 10 as a typical example. It is seen that fragmentation starts at lower energies on the Ni target than on the Au target. Therefore the studied range of beam energy (1.2–2.5 GeV) corresponds for Ni target to the region where the production cross section starts to saturate, whereas for Au target this is region where the production cross section starts to rise quickly. Furthermore, the leveling of the production cross section for the Ni target appears at a lower value than that for the Au target. Both these effects cause that the total production cross sections should rise more quickly for the Au target than for Ni target, in accordance with present observations.

It is interesting to examine how large are the contributions of individual reaction mechanisms for emission of LCPs, i.e., the pre-equilibrium stage of the reaction described by intranuclear cascade and coalescence of nucleons into composite particles,

the fireball emission, and the evaporation. As it is seen in Fig. 11 (right column) the contribution from intranuclear cascade and coalescence is for the Ni target almost equal to that from evaporation and exhausts about 30% of the total production cross section for all studied beam energies and ejectiles. The first of these contributions decreases several percent with the energy, whereas the evaporation contribution (σ_{GEM} on the figure) is almost independent of the energy. The contribution of the fireball is slightly larger ($\sim$40%) and increases several percent in the studied energy range. These variations are more pronounced for tritons and ^{3}He than for protons and deuterons.

This picture is quite different from that of the energy behavior of separate reaction mechanisms of LCPs production for the Au target (cf. Fig. 11, left column), with the exception of the evaporation contribution which is almost energy independent similarly as for Ni target. The coalescence contribution decreases with beam energy ($\sim$10% for p,d,t, and $\sim$30% for ^{3}He) but fireball contribution increases (also $\sim$10% for p,d,t, and even more for ^{3}He). Moreover, the coalescence contribution for Au target is on average larger, and the fireball contribution smaller than for Ni target. Such a behavior of relative contributions of various processes might suggest that they depend rather on the proton beam energy per nucleon of the target than on the beam energy itself, similarly as it is in the case of the total production cross section (cf. Figs. 10 and 11).

V. SUMMARY AND CONCLUSIONS

The aim of the present study was to investigate whether the reaction mechanism observed in Refs. [1,2] for the Au target is also realized in collisions of protons with other target nuclei. The Ni target nucleus was used for this purpose because it has quite different properties than the Au nucleus.

A new, extensive set of double differential cross sections $d^2\sigma/d\Omega dE$ for the production of LCPs and light IMFs (^{6}He, ^{6,7,8}Li, ^{7,9,10}Be, ^{10,11}B, and C) in a collision of protons with the Ni target has been measured at three beam energies (1.2, 1.9, and 2.5 GeV). The spectra of the ejectiles have been determined for seven scattering angles: 16°, 20°, 35°, 50°, 65°, 80°, and 100°.

To facilitate the comparison of the present results with those for a Au target, the analysis of the experimental data was performed using the same method as that applied previously for Au in Refs. [1,2]. The main part of the analysis consisted in searching for best fit parameters of phenomenologically introduced three moving sources emitting isotropically LCPs and IMFs in their rest frame.

An excellent description of all data has been achieved with smoothly varying values of the parameters from ejectile to ejectile. Due to such good reproduction of energy and angular dependencies of $d^2\sigma/d\Omega dE$ by model calculation it was possible to determine total production cross sections for all studied ejectiles. They are listed in Tables I and II for IMFs and LCPs, respectively.

A large contribution of nonequilibrium processes, which are not contained in the two-step microscopic model, has been established. Properties of these processes are compatible with a hypothesis of emission of ejectiles from three moving sources: The light, fast, and hot source (a fireball), which appears as a result of the knock out of a group of nucleons lying on the straight way of the impinging proton through the nucleus, and two slower and colder sources, which are created due to the breakup of the target remnant after the emission of a fireball.

Although the physical interpretation of phenomenologically introduced moving sources is by no means unique, the model was very useful for a systematic comparison of the present data to those measured for the p + Au nuclear system at the same range of beam energies [1,2]. It turned out that all the effects discussed above are very similar in p + Ni and p + Au systems. Since the Ni target is significantly different from Au target (different mass, charge, and N/Z ratio) the observation of analogous reaction mechanisms in both nuclear systems suggests that these phenomena appear generally.[1]

ACKNOWLEDGMENTS

The technical support of A. Heczko, W. Migdał, and N. Paul in preparation of the experimental apparatus is greatly appreciated. This work was supported by the European Commission through European Community-Research Infrastructure Activity under FP6 project Hadron Physics, Contract No. RII3-CT-2004-506078). This work was also partially supported by the Helmholtz Association through funds provided to the virtual institute "Spin and strong QCD" (VH-VI-231). One of us (M.F.) gratefully acknowledges financial support of Polish Ministry of Science and Higher Education (Grant No. N N202 174735, Contract No. 1747/B/H03/2008/35).

[1] Numerical data on the reactions studied in the present work can be found at the PISA collaboration web-page: http://www.fz-juelich.de/ikp/docu/PISA-p-Ni.zip

[1] A. Bubak *et al.*, Phys. Rev. C **76**, 014618 (2007).
[2] A. Budzanowski *et al.*, Phys. Rev. C **78**, 024603 (2008).
[3] R. Barna *et al.*, Nucl. Instrum. Methods Phys. Res. A **519**, 610 (2004).
[4] A. Bubak, B. Kamys, M. Kistryn, and B. Piskor Ignatowicz, Nucl. Instrum. Methods Phys. Res. B **226**, 507 (2004).
[5] G. D. Westfall, R. G. Sextro, A. M. Poskanzer, A. M. Zebelman, G. W. Butler, and E. K. Hyde, Phys. Rev. C **17**, 1368 (1978).
[6] P. Napolitani, K.-H. Schmidt, A. S. Botvina, F. Rejmund, L. Tassan-Got, and C. Villagrasa, Phys. Rev. C **70**, 054607 (2004).
[7] P. Napolitani (private communication).
[8] C.-M. Herbach *et al.*, Nucl. Phys. A **765**, 426 (2006).

[9] G. M. Raisbeck, P. Boerstling, R. Klapisch, and T. D. Thomas, Phys. Rev. C **12**, 527 (1975).
[10] A. Boudard, J. Cugnon, S. Leray, and C. Volant, Nucl. Phys. A **740**, 195 (2004).
[11] S. Furihata, Nucl. Instrum. Methods Phys. Res. B **171**, 251 (2000).
[12] S. Furihata and T. Nakamura, J. Nucl. Sci. Technol. Suppl. **2**, 758 (2002).
[13] A. Letourneau *et al.*, Nucl. Phys. A **712**, 133 (2002).
[14] G. D. Westfall, J. Gosset, P. J. Johansen, A. M. Poskanzer, W. G. Meyer, H. H. Gutbrot, A. Sandoval, and R. Stock, Phys. Rev. Lett. **37**, 1202 (1976).